American Mineralogist, Volume 69, pages 948–953, 1984

A refinement of the crystal structure of gadolinite

Rïtsuro Miyawaki, Izumi Nakai, and Kozo Nagashima

Department of Chemistry
The University of Tsukuba
Ibaraki, 305 Japan

Abstract

The crystal structure of gadolinite has been refined using a spherically ground crystal in the anisotropic mode to a conventional $R = 0.029$ for 2790 independent reflections. Crystal data: monoclinic, space group $P2_1/a$, $a = 10.000(2)$, $b = 7.565(2)$, $c = 4.768(1)$Å, $\beta = 90.31(2)°$, Z = 2. The specimen is from Miyazuma-kyo, Yokkaichi, Japan. Electron microprobe analysis gave the following empirical formula: $RE_{2.00}Fe^{2+}_{0.86}Be_{2.00}Si_{2.00}O_{9.72}(OH)_{0.28}$, suggesting the presence of a vacancy at the Fe site. A consideration of the chemical composition and bond valence sums has indicated the presence of partial substitution of a hydroxyl ion for the oxygen ion compensating for the lack of positive charge at the Fe site. Compositional distribution of the rare earth elements in the specimen is also discussed.

Introduction

Gadolinite has been an important mineral in the history of the discovery of rare earth elements since yttria was first separated by J. Gadolin in 1794.

The ideal formula for gadolinite is expressed as $RE^{3+}_2Fe^{2+}Be_2Si_2O_{10}$, where RE is yttrium and lanthanides. Gadolinite belongs to the datolite–herderite–homilite mineral group. A few other species closely related to gadolinite are known: e.g., calcio-gadolinite ($CaREFe^{3+}Be_2Si_2O_{10}$), in which one half of the RE sites is occupied by calcium (Nakai, 1938) and hingganite found in the USSR ($H_2RE_2Be_2Si_2O_{10}$), where the Fe site is completely vacant (Voloshin et al., 1983).

Ito and Mori (1953) analyzed the structure of datolite and, based on powder diffraction photographs, proposed that the structure of gadolinite can be derived from that of datolite by simple replacement of atoms. This relation was confirmed by Pavlov and Belov (1959) in their structural analysis of gadolinite. However, the analysis was made using two-dimensional photographic data (*hk*0) yielding a fairly large R value of 0.182. Moreover, they mentioned that the analyzed gadolinite specimen gave an X-ray pattern of very poor quality due to the metamict phenomenon, and the chemical composition of the specimen was not considered. Therefore, we undertook the refinement of the structure of gadolinite to obtain a full description of the structure. Gadolinite is known to have close structural relations with datolite and herderite. The crystal structure of datolite was first determined by Ito and Mori (1953), refined by Pant and Cruickshank (1967), and further refined by Foit et al. (1973). That of herderite was determined by Pavlov and Belov (1959) and refined by Lager and Gibbs (1974). In the present investigation, these three structures are compared and discussed in detail.

Chemistry

The gadolinite specimen used in this study is from Miyazuma-kyo, Yokkaichi, Japan (Yamamoto and Nagashima, 1963). To determine the distribution of rare earth elements, chemical analysis was carried out with an electron microprobe. The analysis was made on a JEOL JXA-50A X-ray microanalyzer automated by ELIONIX ACPS-XR control system at the Chemical Analysis Center of the University of Tsukuba.

Analytical conditions are given in Table 1. The accelerating voltage was set at 20 kV, an optimum voltage for lanthanides. The data were corrected using the ZAFN1 program (Z: Duncumb-Reed (Duncumb and Reed, 1968), A: Tanuma-Nagashima (Tanuma and Nagashima, 1983), F: Castaing-Reed (Reed, 1965)).

The results are presented in Table 2. Beryllium was not determined and the molar number was assumed to be equal to that of silicon. Hydrogen atoms were introduced to compensate the charges due to the vacancy at the Fe site. Because of the lack of suitable analytical standards for praseodymium, europium, terbium, and thulium, their wt.% values were estimated from the $L\alpha_1$ peak height ratios of the neighboring lanthanide elements. Thorium was not detected at the accelerating voltages of 20 and 30 kV. The results gave the following empirical formula on the basis of O = 10: $RE_{2.00}Fe^{2+}_{0.86}Be_{2.00}Si_{2.00}O_{9.72}(OH)_{0.28}$.

Figure 1 shows the distribution of lanthanides in the present specimen. The distribution basically follows the

Table 1. Analytical conditions of the electron microprobe analysis

Accelerating voltage	: 20kV
Probe current	: 0.02μA
Beam spot diameter	: 3-5um φ
Analyzing crystals	: RAP Si*K*α PET Ca*K*α, Y*L*α, La*L*α, Ce*L*α, Nd*L*α, Sm*L*α LiF Fe*K*α, Gd*L*α, Dy*L*α, Ho*L*α, Er*L*α, Yb*L*α
Counting times	: 20 sec at peak position 10 sec at both backgrounds
Number of analyzing spot	: 10 spots per a specimen
Analytical standards	: Si - SiO_2 , Ca - $CaSiO_3$ Fe - Fe_2O_3 , Y - $YNbO_4$ La - monazite (natural,analyzed) Ce - monazite (natural,analyzed) Nd - $Nd_3Ga_5O_{12}$, Sm - $Sm_3Ga_5O_{12}$ Gd - Gd(metal), Dy - Dy(metal) Ho - Ho(metal), Er - Er(metal) Yb - Yb(metal)

Table 2. Electron microprobe analysis of gadolinite from Miyazuma-kyo, Japan

	wt%	No. atoms (O=10)
Fe O	12.08	0.864
Mn O	trace	
Y_2O_3	28.55	1.30
La_2O_3	0.21	0.007
Ce_2O_3	2.54	0.080
Pr_2O_3	1.2*	0.036
Nd_2O_3	4.55	0.139
Sm_2O_3	2.82	0.083
Eu_2O_3	0.6*	0.015
Gd_2O_3	2.93	0.083
Tb_2O_3	1.1*	0.032
Dy_2O_3	4.06	0.112
Ho_2O_3	1.98	0.054
Er_2O_3	1.54	0.042
Tm_2O_3	0.2*	0.006
Yb_2O_3	0.58	0.015
Lu_2O_3	trace	
		(ΣRE) 2.00
Ca O	0.03	0.002
Be O **	9.71	2.00
Si O_2	23.36	2.00
H_2O**	0.46	0.272
Total	98.50	

* Estimated from the peak intensities.
** Calculated (See text).

Oddo-Harkins' rule (Oddo, 1914; Harkins, 1917). It is worth noting that neodymium and dysprosium are more abundant than the other lanthanides. The abundance of neodymium is in agreement with the general trend of Japanese gadolinite in which the cerium group elements are relatively rich (Nagashima and Nagashima, 1960). The abundance of dysprosium is due to the fact that yttrium, whose ionic radius is close to that of dysprosium, occupies a large part of the RE site.

Gadolinite often occurs in a metamict state, which may be caused by the presence of such radioactive elements as thorium, isomorphously substituting for the rare earth elements. As mentioned above, the present specimen does not contain any detectable thorium, and it gave X-ray patterns of high quality.

X-ray crystallography

The X-ray powder pattern of gadolinite was obtained on a powder diffractometer at a scan rate of 0.5°/min in 2θ using Ni-filtered Cu$K\alpha$ radiation and Si internal standard (Table 3). Weissenberg photographs showed monoclinic symmetry with systematic absences of the type $h \neq 2n$ for $h0l$ and $k \neq 2n$ for $0k0$ reflections, confirming the space group $P2_1/a$ given by Pavlov and Belov (1959).

A transparent single-crystal fragment of gadolinite was ground into a sphere with the diameter of 0.17 mm, and mounted on a Rigaku AFC-5 four-circle automated diffractometer (X-ray generator: Rotaflex RU200; operating conditions: 50 kV, 160 mA). The lattice parameters, determined by least-squares refinement of the 2θ values of 25 strong reflections, are $a = 10.000(2)$, $b = 7.565(2)$, $c = 4.768(1)$Å, $\beta = 90.31(2)°$, $V = 360.7(1)$Å^3. The intensities were collected on the four-circle diffractometer with graphite-monochromatized Mo$K\alpha$ radiation, 2θ-ω scan technique, at a scan rate of 1°/min. The intensity measurement was repeated for a reflection with $\sigma(|F_0|)/|F_0|$ larger than 0.05. The intensities of three standard reflections measured every 50 observations did not show any fluctuation larger than 2%. The data were corrected for Lorentz, polarization, and absorption factors ($\mu_{MoK\alpha} = 187.0$, calculated based on the chemical composition). The absorption correction was made using ACACA program (Wuensch and Prewitt, 1965). A

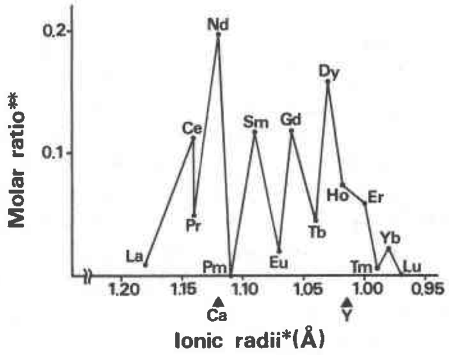

Fig. 1. Compositional distribution of lanthanides in the gadolinite specimen. * Shannon and Prewitt (1969, 1970). ** Molar ratios were normalized so that sum of the molar numbers of lanthanides is equal to one.

Table 3. X-ray powder diffraction data for gadolinite

$h\ k\ l$	$d_{calc.}$	$d_{obs.}$	I/I_0
0 0 1	4.768	4.78	57
2 1 0	4.171	4.17	22
1 2 0	3.538	3.55	22
$\bar{2}$ 0 1	3.460	3.47	27
$\bar{2}$ 1 1	3.146	3.14	73
2 1 1	3.133		
3 1 0	3.050	3.06	30
0 2 1	2.963	2.97	48
$\bar{1}$ 2 1	2.844	2.85	85
1 2 1	2.839	2.84	100
$\bar{3}$ 1 1	2.575	2.58	43
3 1 1	2.564	2.56	50
0 0 2	2.384	2.38	20
4 1 0	2.374	2.37	11
2 3 0	2.252	2.26	12
$\bar{1}$ 1 2	2.220	2.22	16
$\bar{4}$ 0 1	2.219		
$\bar{3}$ 2 1	2.218		
3 2 1	2.211	2.21	12
4 0 1	2.209		
$\bar{1}$ 3 1	2.177	2.18	10
2 3 1	2.034	2.03	16
$\bar{1}$ 2 2	1.979	1.977	20
1 2 2	1.975		
$\bar{3}$ 1 2	1.883	1.883	17
3 1 2	1.874	1.872	15
4 3 0	1.775	1.769	15
2 4 0	1.769		
5 2 0	1.768		
0 4 1	1.758	1.757	12
6 0 0	1.667	1.661	15
6 0 1	1.571	1.568	9

total of 3778 independent reflections were obtained, of which 2790 reflections have a criteria of $|F_0| \geqq 3\sigma(|F_0|)$, and were used for the subsequent crystal structure refinement.

Refinement of the structure

The structure refinement was carried out using the full-matrix least-squares refinement program RFINE2 (Finger, 1969). The atomic coordinates of gadolinite (for x and y) and of datolite (for z) reported by Pavlov and Belov (1959) were used for the initial parameters. The occupancies of yttrium and lanthanides at the RE site were kept at 64.7% and 35.3% respectively, and that of iron was kept at 86.4%, consistent with the chemical composition, throughout all calculations. The scattering factor curve of europium (atomic number: 63, which is close to the weighted average of the atomic numbers for the lanthanides, 62.9, calculated from the chemical composition) was used as that of the lanthanides. The observed structure factors $|F_0|$ were weighted by the formula $1/\sigma^2(|F_0|)$. Iron was fixed at the origin and all the other coordinates were refined. The least-squares refinements were repeated until the shift/error of each parameter became less than 0.01. The structure was refined to $R = 0.055$ and $Rw = 0.062$ with isotropic temperature factors, and $R = 0.029$, $Rw = 0.034$ with anisotropic temperature factors. The final atomic coordinates and temperature factors are listed in Table 4, and observed and calculated

Table 4. Atomic positional parameters and temperature factors, with estimated standard deviations in parentheses

Atom	x	y	z	Beq*	β_{11}	β_{22}	β_{33}	β_{12}	β_{13}	β_{23}
RE	0.32854(2)	0.10828(2)	0.00013(3)	0.62	0.00147(1)	0.00310(2)	0.00619(4)	-0.00020(1)	-0.00050(1)	-0.00007(3)
Si	0.07822(6)	0.27850(9)	0.5192(1)	0.52	0.00129(4)	0.00248(8)	0.0052(2)	-0.00009(5)	-0.00003(7)	-0.0001(1)
Be	0.3355(3)	0.4143(4)	0.4642(6)	0.52	0.0014(2)	0.0024(4)	0.0050(8)	-0.0001(2)	-0.0001(3)	0.0003(4)
Fe	0	0	0	0.67	0.00135(3)	0.00401(7)	0.0061(1)	0.00037(4)	-0.00001(5)	0.00026(8)
O(1)	0.0303(2)	0.4131(2)	0.7607(4)	0.76	0.0020(1)	0.0036(2)	0.0075(5)	0.0003(1)	0.0000(2)	-0.0013(3)
O(2)	0.4518(2)	0.2871(2)	0.3248(4)	0.71	0.0016(1)	0.0036(2)	0.0072(5)	0.0007(1)	-0.0008(2)	-0.0004(3)
O(3)	0.1954(2)	0.3476(3)	0.3089(4)	0.73	0.0014(1)	0.0044(2)	0.0071(5)	-0.0007(1)	-0.0002(2)	0.0013(3)
O(4)	0.1419(2)	0.1065(2)	0.6847(4)	0.72	0.0021(1)	0.0025(2)	0.0083(5)	0.0003(1)	-0.0008(2)	0.0005(3)
O(5)	0.3329(2)	0.4126(3)	0.7979(4)	0.80	0.0020(1)	0.0048(3)	0.0055(4)	-0.0002(1)	0.0002(2)	0.0000(3)

*Beq. is calculated from $4/3(\beta_{11}a^2+\beta_{22}b^2+\beta_{33}c^2+2\beta_{13}ac\cos\beta)$.
The anisotropic temperature factor form is $\exp[-(h^2\beta_{11}+k^2\beta_{22}+l^2\beta_{33}+2hk\beta_{12}+2hl\beta_{13}+2kl\beta_{23})]$.

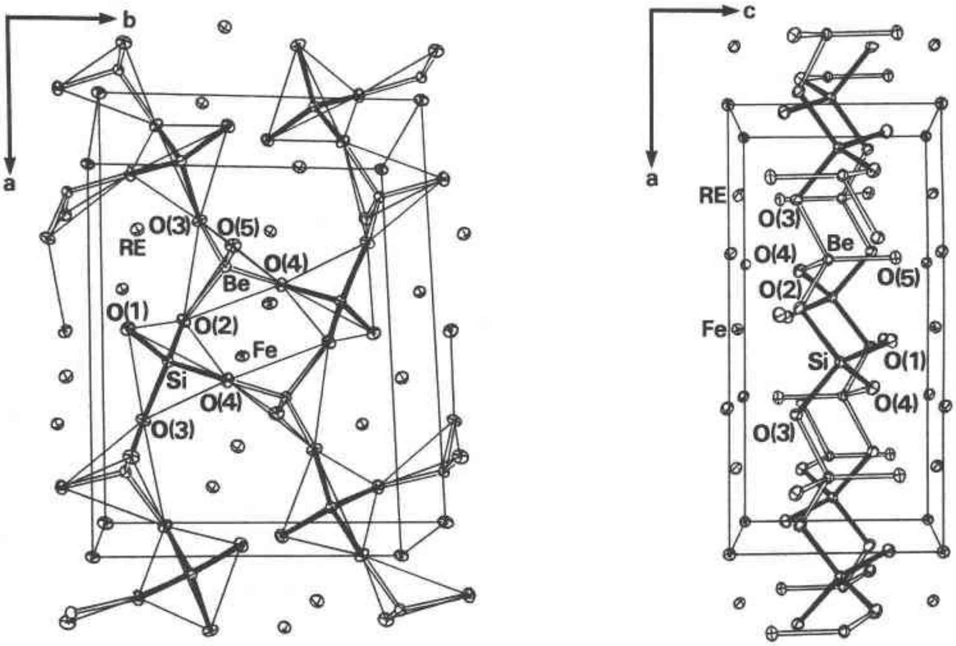

(a) (b)

Fig. 2. Crystal structure of gadolinite. (a) View along **c*** showing the linkage of the SiO_4 and BeO_4 tetrahedra. The tetrahedra are indicated by the single lines. (b) View along **b*** showing the sheet structure made up of the SiO_4 and BeO_4 tetrahedra. The Fe and RE atoms are located at $z \cong 0$, and connect the sheets.

structure factors in Table 5.[1] All the scattering factors were taken from Cromer and Mann (1968), and anomalous dispersion factors from the *International Tables for X-ray Crystallography, Vol. IV* (1974). The calculations were carried out at the Science Information Processing Center of the University of Tsukuba.

Description and discussion of the structure

The crystal structure of gadolinite is illustrated in Figure 2. The structure can be described in terms of a sheet structure built up from alternating SiO_4 and BeO_4 tetrahedra. The sheet extends parallel to the (001) plane at $z \cong 0.5$. The rare earth and iron atoms are located at $z \cong 0$, and connect the sheets. The silicon atom exhibits the usual tetrahedral coordination by four oxygen atoms, O(1), O(2), O(3), and O(4). Similarly, the beryllium atom is tetrahedrally coordinated by four oxygen atoms, O(2), O(3), O(4), and O(5). These tetrahedra make corner-sharing linkages at O(2), O(3), and O(4) sites to form the sheet structure. This structural feature is consistent with that reported by Pavlov and Belov (1959).

The interatomic distances and bond angles were calculated using UMBADTEA (Finger and Prince, 1975) and are listed in Table 6, together with those for datolite (Foit et al., 1973) and herderite (Lager and Gibbs, 1974) for comparison. As suggested by Ito and Mori (1953), and later confirmed by Pavlov and Belov (1959), the structure of gadolinite can be derived from that of datolite simply by replacing calcium with yttrium, boron with beryllium, and OH with oxygen, and, in addition, placing iron at (0,0,0). The structure of herderite is isotypic with that of datolite (Pavlov and Belov, 1959). Table 7 summarizes the relevant data for the three structures used in the subsequent comparison.

As is commonly observed in silicate structures, the non-bridging Si–O(1) bond, of length 1.612(2)Å is shorter than the other three bridging Si–O bonds, of mean length 1.640Å. However, the difference in the length between non-bridging and bridging Si–O bonds is not so large as the difference observed in datolite, 0.083Å, (Foit et al., 1973).

In the BeO_4 tetrahedron, the non-bridging Be–O(5) bond, of length 1.592(3)Å, is also shorter than the bridging Be–O bonds, of mean length 1.648Å. This is not observed in datolite and herderite where the O(5) positions are occupied by different anions (OH^-).

The RE site, which is occupied by many different kinds of rare earth elements, is surrounded by eight oxygen atoms (Fig. 3(a)). Pant and Cruickshank (1967) mentioned that the considerable strength of Ca–O bonds accounts for the lack of cleavage in datolite in spite of its sheet

---

[1] Table 5 may be obtained by ordering Document Am-84-249 from the Business Office, Mineralogical Society of America, 2000 Florida Ave., N.W., Washington, D.C., 20009. Please remit $5.00 in advance for the microfiche.

Table 6. Interatomic distances (Å) and bond angles (°) with estimated standard deviations in parentheses. The values for datolite and herderite are also given for comparison

gadolinite*	datolite**	herderite***
Distances (Å)		
RE-O1 2.329(2)	Ca-O1 2.276(2)	Ca-O1 2.375(3)
-O1' 2.335(2)	-O1' 2.280(2)	-O1' 2.369(3)
-O2 2.392(2)	-O2 2.453(2)	-O2 2.459(3)
-O3 2.473(2)	-O3 2.607(2)	-O3 2.616(3)
-O3' 2.691(2)	-O3' 2.658(2)	-O3' 2.741(3)
-O4 2.381(2)	-O4 2.420(2)	-O4 2.439(3)
-O5 2.497(2)	-O5 2.672(2)	-OH 2.418(3)
-O5' 2.397(2)	-O5' 2.518(2)	-OH' 2.509(3)
Si-O1 1.612(2)	Si-O1 1.570(2)	P -O1 1.513(3)
-O2 1.641(2)	-O2 1.648(2)	-O2 1.543(3)
-O3 1.632(2)	-O3 1.651(2)	-O3 1.552(3)
-O4 1.648(2)	-O4 1.661(2)	-O4 1.554(3)
Be-O2 1.651(3)	B -O2 1.475(3)	Be-O2 1.630(5)
-O3 1.660(3)	-O3 1.486(3)	-O3 1.651(5)
-O4 1.634(4)	-O4 1.464(3)	-O4 1.610(5)
-O5 1.592(3)	-O5 1.496(3)	-OH 1.602(5)
Fe-O2 2.288(2)×2	ORG†-O2 2.188×2	ORG†-O2 2.389×2
-O4 2.224(2)×2	-O4 2.178×2	-O4 2.266×2
-O5 2.035(2)×2	-O5 2.117×2	-OH 2.020×2
Angles (°)		
O1-Si-O2 111.33(9)	O1-Si-O2 113.95(8)	O1- P -O2 111.4(1)
O1-Si-O3 116.96(10)	O1-Si-O3 115.26(8)	O1- P -O3 112.9(1)
O1-Si-O4 105.81(9)	O1-Si-O4 108.69(8)	O1- P -O4 108.9(1)
O2-Si-O3 107.67(9)	O2-Si-O3 106.74(8)	O2- P -O3 107.9(1)
O2-Si-O4 109.04(10)	O2-Si-O4 106.15(8)	O2- P -O4 109.0(1)
O3-Si-O4 105.67(9)	O3-Si-O4 105.34(8)	O3- P -O4 106.6(1)
O2-Be-O3 103.8(2)	O2- B -O3 107.9(2)	O2-Be-O3 107.0(3)
O2-Be-O4 103.2(2)	O2- B -O4 109.5(2)	O2-Be-O4 110.5(3)
O2-Be-O5 114.4(2)	O2- B -O5 111.1(2)	O2-Be-OH 111.3(3)
O3-Be-O4 101.3(2)	O3- B -O4 106.9(1)	O3-Be-O4 103.7(3)
O3-Be-O5 115.2(2)	O3- B -O5 109.4(2)	O3-Be-OH 109.8(3)
O4-Be-O5 116.4(2)	O4- B -O5 111.9(2)	O4-Be-OH 114.0(3)
O2-Fe-O4 70.11(7)		
O2-Fe-O4' 109.89(7)		
O2-Fe-O5 85.20(7)		
O2-Fe-O5' 94.80(7)		
O4-Fe-O5 84.99(7)		
O4-Fe-O5' 95.01(7)		

* Present study.
** Foit, Phillips, and Gibbs (1973).
*** Lager and Gibbs (1974).
† Origin.

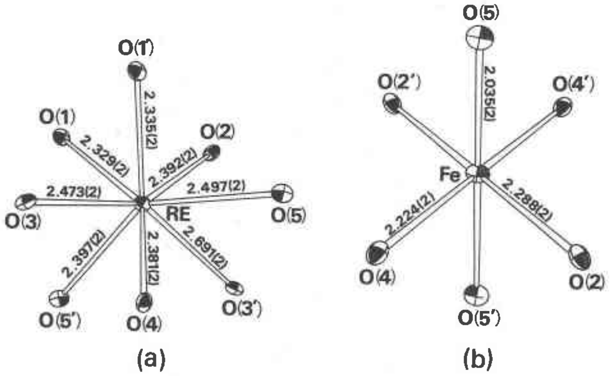

Fig. 3. Coordination polyhedra in gadolinite, showing ellipsoids of thermal vibration: (a) REO$_8$ polyhedron. (b) FeO$_6$ octahedron.

structure. Similarly the RE–O bonds (see Table 8) account for the absence of cleavage in gadolinite.

The iron atom and oxygen atoms form a distorted octahedron showing the Jahn–Teller effect (Fig. 3b). The average Fe–O distance, 2.182Å, is nearly equal to the sum of the ionic radii of Fe^{2+} and O^{2-} (Shannon and Prewitt, 1969, 1970), 0.78 + 1.40 = 2.18Å. Although the presence of iron in gadolinite gives a clear compositional distinction from datolite and herderite, the role of iron in the structure does not seem to be very significant. The average Fe–O distance, 2,182Å, is close to the corresponding origin-oxygen distance in datolite, 2.161Å (Table 6). Moreover, there are vacancies at the Fe sites in the present specimen and, as the extreme case, hingganite, $H_2RE_2Be_2Si_2O_{10}$, has been shown to have the Fe sites completely vacant (Voloshin et al., 1983).

The chemical composition of the investigated specimen (Table 2) has suggested the presence of hydroxyl anions partially substituting for oxygen. In order to predict the anion chemistry and bond strengths, the bond valence

Table 7. Crystallographic data for gadolinite, datolite, and herderite

	gadolinite*	datolite**	herderite***
Formula unit	$RE^{3+}_2Fe^{2+}Be_2Si_2O_{10}$	$CaBSiO_4(OH)$	$CaBePO_4(OH)$
Crystal system	monoclinic	monoclinic	monoclinic
Space group	$P2_1/a$	$P2_1/a$	$P2_1/a$
a	10.000(2) Å	9.636(8) Å	9.789(2) Å
b	7.565(2)	7.608(4)	7.661(1)
c	4.768(1)	4.832(4)	4.804(1)
β	90.31(2)°	90.40(7)°	90.02(1)°
Z	2	4	4

* Present study.
** Foit, Phillips, and Gibbs (1973).
*** Lager and Gibbs (1974).

Table 8. Valence balance of gadolinite

	RE	Si	Be	Fe^{2+}	$\Sigma C\upsilon$	Anion chemistry
O(1)	0.45 0.44	1.04			1.93	O^{2-}
O(2)	0.41	0.98	0.47	0.20	2.06	O^{2-}
O(3)	0.22 0.35	1.00	0.47		2.04	O^{2-}
O(4)	0.41	0.96	0.50	0.25	2.12	O^{2-}
O(5)	0.34 0.40		0.57	0.47	1.78	O^{2-},OH^-
$\Sigma A\upsilon$	3.02	3.98	2.01	0.92 (×2)		

sums were calculated using the values of the bond lengths and coordination numbers according to the method of Donnay and Allmann (1970) (Table 8). The bond valence sum calculated for O(5), 1.78, indicates a substantial deviation from the ideal value of 2 for the oxygen ion. This suggests partial substitution for the oxygen ion by a hydroxyl ion at the O(5) site. The presence of vacancies at the Fe sites accompanying the charge compensation by the substitution of a hydroxyl ion for the oxygen ion may support the idea suggested by Ito and Hafner (1974), namely that naturally occurring boron-free gadolinites are solid-solutions in a three component system of the type gadolinite ($RE_2Fe^{2+}Be_2Si_2O_{10}$)–calcio-gadolinite ($CaREFe^{3+}Be_2Si_2O_{10}$)–hingganite ($H_2RE_2Be_2Si_2O_{10}$).

Acknowledgments

The authors are grateful to Mr. N. Nishida for his kind advice concerning electron microprobe analysis and to Mr. K. Kakefuda for the maintenance of the four-circle diffractometer. The figures of the crystal structures were drawn with the ORTEP program (Johnson, 1965).

References

Cromer, D. T. and Mann, J. B. (1968) X-ray scattering factors computed from numerical Hartree-Fock wave functions. Acta Crystallographica, A24, 321–324.

Donnay, G. and Allmann, R. (1970) How to recognize O^{2-}, OH^-, and H_2O in crystal structures determined by X-rays. American Mineralogist, 55, 1003–1015.

Duncumb, P. and Reed, S. J. B. (1968) Quantitative electron probe microanalysis. In. K. F. J. Heinrich, Ed., National Bureau of Standards Special Publication, No. 289. Washington, D.C.

Finger, L. W. and Prince, E. (1975) National Bureau of Standards Technical Note 854, 54–55. U.S. Government Printing Office, Washington, D.C.

Finger, L. W. (1969) Determination of cation distribution by least-squares refinement of single-crystal X-ray data. Carnegie Institution Year Book, 67, 216–217.

Foit, F. F., Phillips, M. W., and Gibbs, G. V. (1973) A refinement of the crystal structure of datolite, $CaBSiO_4(OH)$. American Mineralogist, 58, 909–914.

Harkins, W. D. (1917) The evolution of the elements and the stability of complex atoms. Journal of the American Chemical Society, 39, 856–879.

International Tables for X-ray Crystallography, Vol. IV (1974). p. 148–150. Kynoch Press, Birmingham, England.

Ito, J. and Hafner, S. S. (1974) Synthesis and study of gadolinites. American Mineralogist, 59, 700–708.

Ito, T. and Mori, H. (1953) The crystal structure of datolite. Acta Crystallographica, 6, 24–32.

Johnson, C. K. (1965) ORTEP: a FORTRAN thermal-ellipsoid plot program for crystal structure illustrations. Oak Ridge National Laboratory Report ORNL-3794 (second revision, 1970).

Lager, G. A. and Gibbs, G. V. (1974) A refinement of the crystal structure of herderite, $CaBePO_4(OH)$. American Mineralogist, 59, 919–925.

Nagashima, O. and Nagashima, K. (1960) Rare element minerals from Japan, p. 184–189. Japan Mineral Club Press, Kyoto, Japan.

Nakai, T. (1938) On calciogadolinite, a new variety of gadolinite found in Tadachi, Nagano, Japan. Bulletin of the Chemical Society of Japan, 13, 591–594.

Oddo, G. (1914) Die Molekularstruktur der radioaktiven Atome. Zeitschrift für Anorganische und Allgemeine Chemie, 87, 253–268.

Pant, A. K. and Cruickshank, D. W. J. (1967) A reconsideration of the structure of datolite, $CaBSiO_4(OH)$. Zeitschrift für Kristallographie, 125, 286–297.

Pavlov, P. V. and Belov, N. V. (1959) The structure of herderite, datolite, and gadolinite determined by direct methods. Kristallographiya, 4, 324–340.

Reed, S. J. B. (1965) Characteristic fluorescence correction in electron-probe microanalysis. British Journal of Applied Physics, 16, 913–926.

Shannon, R. D. and Prewitt, C. T (1969) Effective ionic radii in oxides and fluorides. Acta Crystallographica, B25, 925–945.

Shannon, R. D. and Prewitt, C. T. (1970) Revised values of effective ionic radii. Acta Crystallographica, B26, 1046–1048.

Tanuma, S. and Nagashima, K. (1983) Evaluation of an improved absorption correction based on the Gaussian ionization distribution model for quantitative electron probe microanalysis. Mikrochimica Acta, 1983, 299–313.

Voloshin, A. B., Pakhomovskii, Ia. A., and Menshikov, Iu. P. (1983) Hingganite-(Yb), a new mineral from amazonite pegmatite in the Kola Peninsula. Doklady Akademii Nauk USSR, 270, 1188–1192.

Wuensch, B. J. and Prewitt, C. T. (1965) Corrections for X-ray absorption by a crystal of arbitrary shape. Zeitschrift für Kristallographie, 122, 24–59.

Yamamoto, S. and Nagashima K. (1963) Gadolinite from Miyazuma-kyo, Yokkaichi, Japan. Chigaku-kenkyu, 1963, 130–133.

Manuscript received, September 27, 1983;
accepted for publication, May 1, 1984.